Journal Name

ARTICLE

Photochromic performances of two Cu(II)-1D solvatomorphs controlled by intermolecular interactions†

Received 00th January 20xx,
Accepted 00th January 20xx

DOI: 10.1039/x0xx00000x

www.rsc.org/

Jorge Salinas Uber,[a] Marta Estrader[a,*] Corine Mathonière,[b,c] Rodolphe Clérac,[d,e] Olivier Roubeau[f] and Guillem Aromí[a,*]

One of the benefits found in crystal engineering to built molecular materials is the possibility of understanding, and thus finely controlling their photochromic performance in the solid state. We have discovered potential hints in this direction through the use of the photochromic ligand 1,2-bis(5-carboxy-2-methylthien-3-yl)cyclopentene, H_2L, in reactions with either of two Cu(II) salts for the formation of two new solvatomorphs of a coordination polymer, $[Cu(L)(py)_3]\cdot 2py$ (**1a**) and $[Cu(L)(py)_3]\cdot 2H_2O\cdot 0.5Et_2O$ (**1b**). H_2L is a diarylethene ligand that exhibits reversible photocyclization, potentially allowing to reversibly modifying the exchange coupling between paramagnetic species separated by such moiety. While the backbone of both compounds is the same, their supramolecular organization significantly differs, leading to different photochromic properties, in particular regarding the reversibility of their photoswitching processes. These remarkable structure/property relations have been assessed by optical reflectivity and Raman measurements, in light of the respective crystallographic structures.

Introduction

Molecular structures assembled by organic photochromic systems may be excellent candidates as main components of molecular photo-switching devices and biomaterials.[1-13] Reversible photo-isomerization processes lead to changes in physico-chemical properties such as absorption spectra,[5] magnetic behaviour,[14, 15] electron conductivity,[16, 17] fluorescence[18] or crystal morphology,[19, 20] to mention only a few. Among the photochromic molecules, diarylethene-based systems are among the most promising compounds. In addition to their chemical and structural versatility, they undergo reversible photo-cyclization processes with high thermal stability and quantum yield as well as with an excellent resistance to fatigue (Scheme I).[21] One of the compulsory conditions for the formation of the C–C bond in this process is that the aryl rings must be in the antiparallel conformation, in order to avoid the steric hindrance between their methyl groups upon the ring closure. It has been now established that this photoisomerization can take place either in solution or in the solid state.[19] The complexity generally associated to solid state photochemistry has attracted attention recently. Unlike in solution, molecules within a lattice are interconnected and kept in fixed positions, therefore, their photoconverting properties could be easily influenced by small changes to the intermolecular interactions and the crystal packing.[22, 23] Regarding metal complexes based on diarylethene ligands, although most of the work has been devoted to organometallic multifunctional materials combining the photo- and electro-chromic properties,[24-27] a few reports related to photomagnetism are also available.[15, 28-33] However, little attention has been paid to crystal engineering of photoactive coordination systems, in other words to study the crystal packing requirements to perform the photoisomerization in the solid state. Along this line, some studies report on the photochromism of metal complexes in the crystalline phase[15, 30-35] while no examples are found assessing differences in photoactivity behaviour between two polymorphic compounds.

Despite the widespread research on diarylethene derivates, these materials are indeed, mainly based on the diarylper-

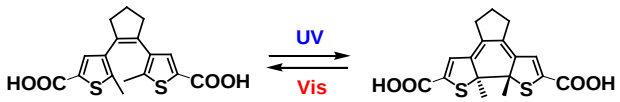

Scheme 1. Representation of the **H_2L** ligand and its reversible photocyclization. with $\lambda_{UV} < 400$ nm and $\lambda_{Vis} > 450$ nm.

[a] Departament de Química Inorgànica, Universitat de Barcelona, Diagonal 645, 08028, Barcelona, Spain.
[b] CNRS, ICMCB, UPR 9048, F-33600 Pessac, France.
[c] Univ. Bordeaux, ICMCB, UPR 9048, F-33600 Pessac, France.
[d] CNRS, CRPP, UPR 8641, 33600 Pessac, France.
[e] Univ. Bordeaux, CRPP, UPR 8641, 33600 Pessac, France.
[f] Instituto de Ciencia de Materiales de Aragon (ICMA) and Departamento de Física de la Materia Condensada, CSIC and Universidad de Zaragoza, E-50009 Zaragoza, Spain.

† *Electronic Supplementary Information (ESI) available: additional structural, optical reflectivity and magnetic data. See DOI: 10.1039/x0xx00000x*

fluoropentene entity. The synthesis of these compounds is neither trivial nor easy to scale up since they used octafluorocyclopentene as reagent, which is very volatile and expensive while the yields are very low. To solve these problems, Feringa *et al.* reported a new synthetic pathway where a perhydro-cyclopentene unit was used instead of the perfluoro analogue.[36] Interestingly, although this procedure is cheaper and allows large scale reactions, only few coordination complexes based on these derivatives can be found in the literature.[4, 26, 37-39]

We report here two solvatomorphs of a Cu(II) coordination polymer, $[Cu(L)(py)_3]$ (**1**), where $\mathbf{H_2L}$ is the fluorine-free photochromic ligand 1,2-(5-carboxy-2-methyl-thiophen-3-yl)-cyclopentene (Sheme I). Both compounds feature polymeric chains alternating pyridine bound Cu(II) ions and L^{2-} ligands acting as bridging units through their carboxylate functionalities. The crystal packing of these chains is quite different due to the presence of dissimilar guest molecules. As a consequence, although both solvatomorphs are photoactive, the kinetics of the process is drastically different. The reversible photoconversion in the crystalline phase for both complexes has been characterized by means of optical reflectivity and Raman spectroscopy techniques. Moreover, the magnetic properties of both compounds have also been assessed. The distinct behaviour is rationalized in light of the structural information.

Results and discussion

Synthesis and Molecular Structures

Compounds **1a** and **1b** are solvathomorphs of the same coordination complex, formed as slightly different isomers (see below). The composition of their crystal lattice is $[Cu(L)(py)_3]\cdot 2py$ (**1a**) and $[Cu(L)(py)_3]\cdot 2H_2O\cdot 0.5Et_2O$ (**1b**), respectively, thus just differing in the nature of the solvent molecules of crystallization. While both reactions were performed through the exact same procedure and using the same solvents, the only distinction was the initial source of Cu(II) metal ions: $Cu(AcO)_2\cdot H_2O$ and $Cu(NO_3)_2\cdot 3H_2O$ for **1a** and **1b**, respectively. Interestingly however, the different counter ions are not present in the final products. Therefore, the reasons for a different final composition and solid state arrangement (see below) may have to do with the role that AcO^- and NO_3^- play on the equilibria taking place in solution, or with the larger amount of water borne by the nitrate salt. Both procedures were found to be fully reproducible.

Compounds **1a** and **1b** crystallize in the monoclinic space group $P2_1/c$ (Table S1). Their asymmetric unit (Fig. S1) coincides with their empirical formulae, and the unit cell contains four such units. Selected metric parameters are listed in Tables S2 and S3. Both compounds consist of polymeric chains of Cu(II) ions linked by the L^{2-} ligands through their end carboxylate groups acting as monodentate donors on each Cu site (Fig. 1 and S2). Thus the unique Cu site exhibits two *trans* Cu–O bonds (distances: 1.954 and 1.973 Å, **1a**; 1.950 and 1.954 Å, **1b**).

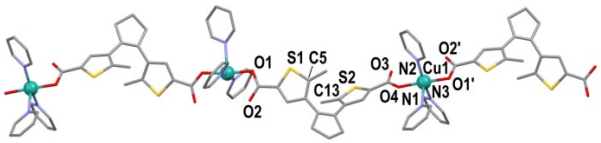

Figure 1. Representation of the polymeric chain of **1a** with heteroatoms of the asymmetric unit (and some symmetry equivalent) labelled. The polymeric chain of **1b** is very similar (see figure S2).

The Cu···O distances to the other oxygen atoms of the carboxylate groups diverge more for complex **1a** (2.768 and 3.322 Å) than for **1b** (2.982 and 3.023 Å). Additionally, each metal ion is coordinated by three solvent pyridine molecules in a *mer* fashion. The Cu(II) ions are thus described as five coordinate (N_3O_2) with slightly distorted trigonal bipyramidal geometries. In **1a**, the axial site is occupied by a pyridine molecule that exhibits occupational disorder over two positions (0.73:0.27 ratio). In **1b**, the axial pyridine group is fully ordered. In both compounds, the coordination polyhedron around Cu(II) alternates within the chain between two approximately opposite orientations, the $Cu–N_{axial}$ angle between both orientations being 150.56° and 119.58° for **1a** and **1b**, respectively. The cyclopentene unit of the photochromic spacer alternates as well between two almost opposite orientations (Fig. S2). In both cases, the chains are not chiral, since both enantiomeric conformers of the $\mathbf{L^{2-}}$ ligand are present and alternate within the chains. The crystal packing of compound **1a** shows a two-dimensional arrangement of the chains linked by π–π stacking interactions between the equatorial pyridine molecules (inter-centroid distance of 3.586 Å; Fig. S3). Within the sheets, the inter-chain connected Cu centers exhibit the exact same mutual orientation, as do adjacent diarylethene units. The free space available between chains is shaped as infinite channels efficiently occupied by a 1D supramolecular array of pyridine molecules connected by a combination of π–π stacking and C–H···π interactions (Fig. 2 and S4). The chains of **1b** also organize as 2D assemblies (Fig. S5) through lateral π–π stacking interactions involving equatorial pyridine ligands (inter-centroid distance of 3.663 Å, Fig. S5). Here however, adjacent Cu(II) ions between chains exhibit opposite

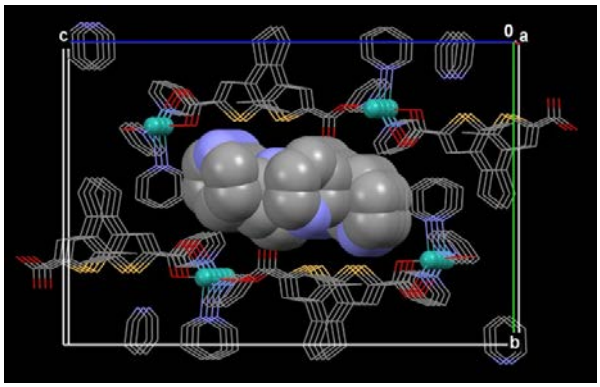

Figure 2. Ball and stick representation two stacks of polymeric chains of **1a**, *quasi* down the crystallographic *a* axis, forming two adjacent sheets and emphasizing the 1D channels parallel to *a* traversing through the middle of the unit cell. The latter are occupied by ordered molecules of pyridine molecules (here in the spacefill style).

orientations, as do adjacent diarylethene units. This arrangement conduces to 2D sheets that are much more corrugated than in **1a** and also prevents the establishment of 1D channels as seen in the other compound. Instead, two types of cavities are formed in between the sheets (Fig. S6); *i*) one with a hydrophobic character that contains one half disordered molecule of ether and *ii*) one hydrophilic that sees four non-coordinated carboxylate O-atoms pointing towards its interior forming a total of six hydrogen bonds with four hosted water molecules (Fig. S7). This network of hydrogen bonds contributes to the cementing of the 2D sheets of **1b** within the tridimensional lattice. In both compounds, the thiophenyl rings within the photoswitchable unit exhibit an antiparallel arrangement, a necessary condition for the photochromic conversion to proceed.[20] Another important parameter in this respect is the distance between the C-atoms that form a new bond during the cyclisation process, which needs to be shorter than approximately 4 Å.[40] This distance is 3.550 Å and 3.479 Å for **1a** (C5···C13) and **1b** (C20···C30), respectively.

Photoswitching Properties

The photoisomerization properties of compounds **1a** and **1b** in the solid state were examined through optical reflectivity and Raman spectroscopic measurements.

Optical Reflectivity Measurements

The photoswitching properties of **H_2L**, **1a** and **1b** were investigated by optical reflectivity in the solid state (in the 400 - 900 nm range). As a preliminary experiment, the variable temperature optical reflectivity of the **H_2L** ligand in its opened form was determined (Fig. S8), which showed almost no spectral variations with temperature. When a powdered sample of **H_2L** was irradiated continuously with UV light (365 nm) at 290 K, the pale brown solid of the opened form turned deep violet as expected in presence of the closed isomer. This change of colour can be followed during approximately 2 hours as a clear decrease of the absolute reflectivity, most noticeable in the 450 to 650 nm region where a broad band appears progressively (Fig. 3A). After 4.5 hours of irradiation, practically no further evolution could be observed (Fig. 3C, *vide infra*). Then, the thermal variation of the optical reflectivity properties of the irradiated/closed product was also studied (Fig. S9), and showed again almost no variation with temperature. If the compound is then irradiated with visible light (455 nm and 530 nm) at room temperature, the photoconversion of **H_2L** is reversed partially (with 530 nm light) or totally (with 455 nm light), as followed again through absolute reflectivity (Fig. 3B and S10). The kinetics and reversibility of both photochromic **H_2L** reactions were studied at 295 K through the time dependence of the absolute reflectivity at a specific wavelength (selected here at 500 nm), irradiating with light of 365 nm for the direct process and of 455 nm for the reverse isomerization (Fig. 3C). The absolute reflectivity at 500 nm rapidly decreases from 0.40 to 0.06

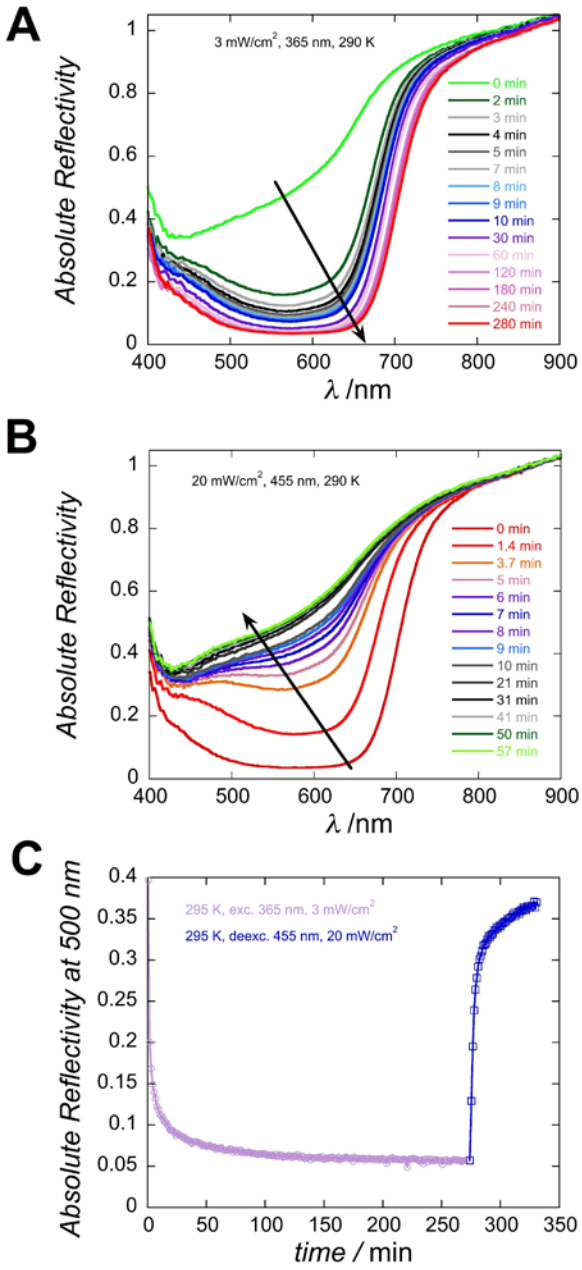

Figure 3. Evolution of the absolute reflectivity for **H_2L** upon continuous irradiation at 295 K with (A) 365 nm light (3 mW/cm²) and subsequently (B) 455 nm light (20 mW/cm²). (C) Same data plotted as the time evolution of the absolute reflectivity at 500 nm during the two consecutive irradiations.

under 365 nm excitation, while it increases again upon excitation with 455 nm light, to reach in about 50 min the value of 0.36. To the best of our knowledge, the optical properties of **H_2L** in the solid state have not been previously reported. Nevertheless, the noticeable decrease of optical reflectivity of this compound in the 450-650 nm range is consistent with previously observed changes to its solution absorption spectra upon irradiation with UV light.[36] The latter mainly consist on the development of a broad band centred at 530 nm attributed to π···π* transitions through the conjugated skeleton.[36] Indeed, the solution and solid state spectral behaviour may not change significantly, as

already observed for a molecule analogous to **H_2L**, with a perfluoropentene instead of a pentene unit.[23]

The same experimental protocol was carried out for compounds **1a** and **1b**. First, reflectivity experiments were performed in order to determine the temperature dependence of the spectra of both complexes (Figs. S11 and S12). Both **1a** and **1b** display strong absorptions above 700 nm due to the d-d transitions centred on the Cu^{2+} ions. Besides, more pronounced thermal changes than observed for **H_2L** (Fig. S8 and S9) were detected, reflecting on a larger temperature influence of the near infrared transitions, more enhanced for **1b** (Figs. S11 and S12). These thermal variations are fully reversible. For complex **1a**, irradiation with UV light (λ = 365 nm) causes a decrease of the reflectivity that is most obvious in the 450-600 nm range (Fig. 4A), which may be attributed to the formation of the closed form isomer. A steady state was reached after approximately 90 minutes of irradiation. The thermal variation of the reflectivity properties of the irradiated/closed form were also examined (Fig. S12), and similarly to the open form, the variations were fully reversible. Subsequently, the reverse photoconversion to the original opened form was investigated with different wavelengths: λ = 625, 590, 530 and 455 nm (Fig. S14). Only the green light (λ = 530 nm) was active to reverse the photoisomerisation process (Fig. 4B). Actually, time dependence studies of the absolute reflectivity during the excitation-de-excitation cycle reveal that the reversibility is only partial as the initial absolute reflectivity is not fully recovered (Fig. 4C). It is conceivable that the first isomerization causes changes to the crystal lattice that prevent the restoration of the exact original system. Quite remarkably, complex **1b** shows a totally different behaviour. First, it requires fivefold longer UV irradiation times (approximately eight hours) than **1a** to reach a photostationary state, presumably corresponding to the closed form (Fig. 5A). Secondly, the associated reverse process was not observed (Fig. 5B). Note that several attempts with other wavelengths in the visible range did not lead to reversibility for **1b**. The failure to cause any reverse conversion may be attributed to changes of the crystal structure after the closure of the diarylethene, blocking the reverse process. The resulting system also exhibits a thermal dependence of the absolute reflectivity (Fig. S15) similar to that of the original sample. The different optical and photoconversion properties for both coordination polymers must be rooted on their crystalline arrangement. One difference is that the layers made of chains in **1b** are packed through a network of H-bonding interactions (mediated by water molecules) that is absent in **1a**. This may render the molecular rearrangement and the lattice more rigid and thus more difficult to adapt to the photocyclization for **1b** than for **1a**. It is possible that the parallel disposition of adjacent chains in **1a** (*vide supra*, Fig. S3) are preserved in both of its forms. The dramatic difference between the photoactivity kinetics of the two compounds suggests that the alternating arrangement in **1b**

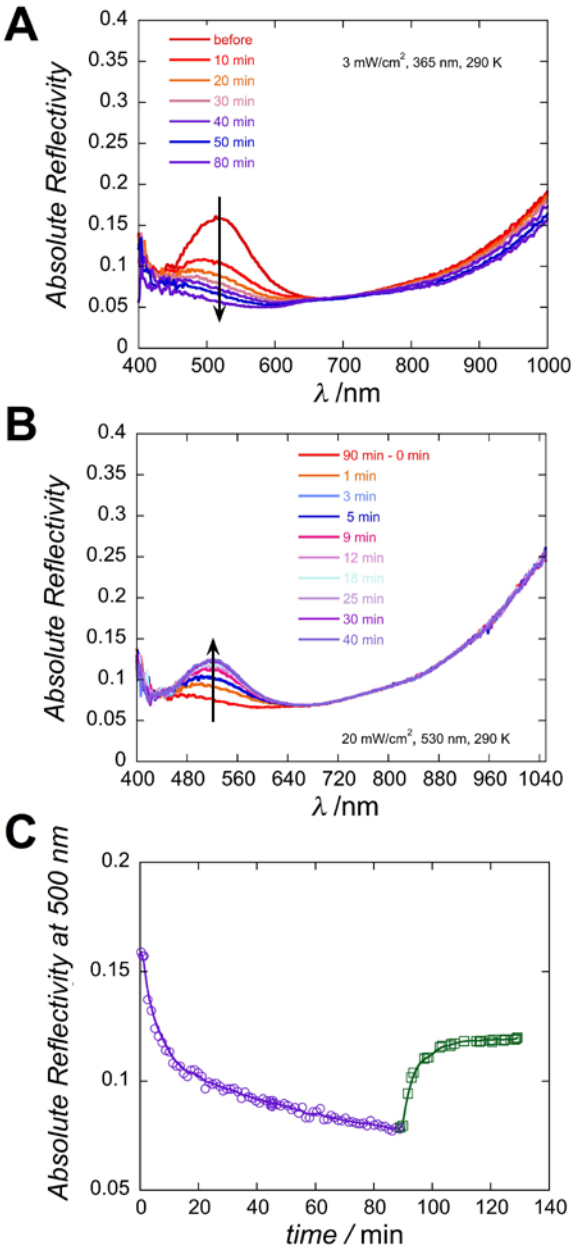

Figure 4. Evolution of the absolute reflectivity for **1a** upon continuous irradiation at 290 K with (A) 365-nm light (3 mW/cm²) and subsequently (B) 455-nm light (20 mW/cm²). (C) Same data plotted as the time evolution of the absolute reflectivity at 500 nm during the two consecutive irradiations.

does not facilitate the concerted atomic movement throughout the lattice required for the reversible photoconversion.

It must be noted that, to the best of our knowledge, there are no reported studies about the role of the supramolecular arrangement on the photochromic properties of metal complexes assembled by diaryelethene ligands. However, some papers report on the quenching or the appearance of photoconversion in diarylethene single crystals depending on the exact crystal structure. For instance, an increase of the quantum yield of up to 100 % can be achieved by introducing guest molecules (favouring

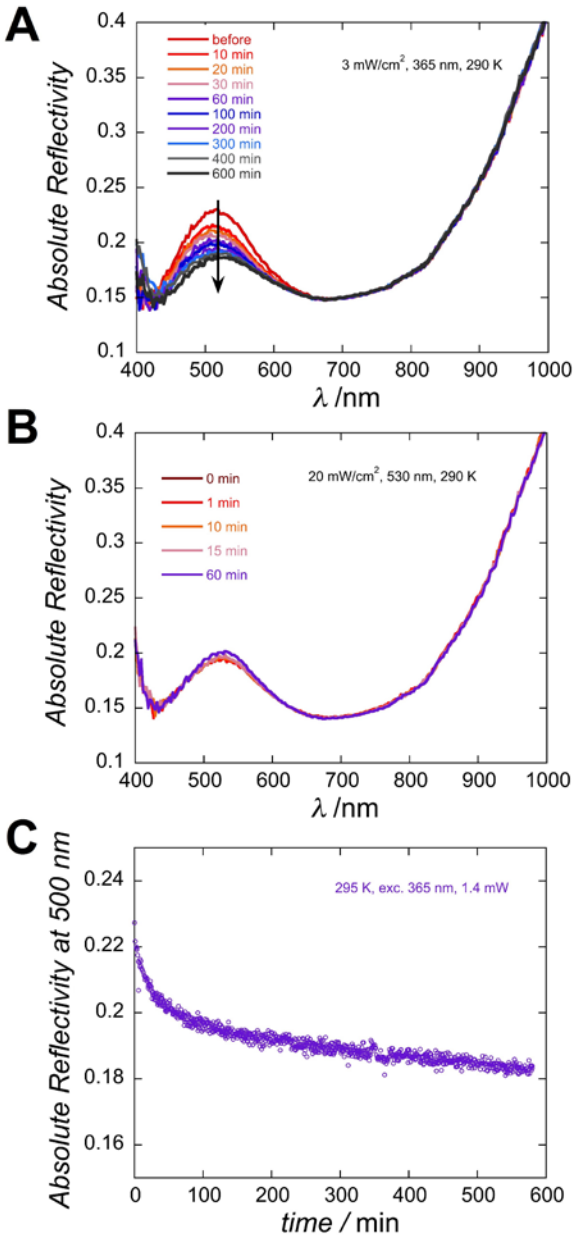

Figure 5. Evolution of the absolute reflectivity for **1b** upon continuous irradiation at 295 K with (A) 365-nm light (3 mW/cm^2) and subsequently (B) 455-nm light (20 mW/cm^2). (C) Same data plotted as the time evolution of the absolute reflectivity at 500 nm during the two consecutive irradiations.

the antiparallel arrangement of thiophenyls via intermolecular interactions) into the lattice.[22, 23, 41]

Raman spectroscopy

The **H_2L** ligand and its Cu(II) complex **1a** exhibit Raman spectra similar to that of other previously studied bisthiophenylethene derivatives (Fig. 6).[42, 43] Spectra on powdered samples of both compounds were then recorded after subsequent and repeated cycles of continuous UV light irradiation (< 425 nm). During the course of this irradiation, the colour of the illuminated area changes in the same way as was observed during the optical reflectivity experiments. This process however, does not result in large spectral Raman changes. However, as seen on previous compounds,[44] the appearance of a distinct band near 1500 cm^{-1} upon photo-isomerization is very obvious and constitutes a marker of the ring closure. Importantly, the reversal of the process by illumination with visible light (> 430 nm) takes place indeed with complete disappearance of this marker, which is consistent with the reflectivity results for **H_2L** and **1a**. This peak is attributed to a C=C stretching vibration of the thiophene unit when it becomes embedded within the extended conjugated polyenic structure of the closed form.[43-45] Regarding complex **1b**, the experiments were hampered by the weakness of the signal. This is ascribed to the instability of the sample under the Raman beam excitation. This confirms once again the dramatic differences in photo-responsive behaviour of both solvatomorphs.

Bulk magnetic measurements

The variable temperature bulk magnetic susceptibility of complexes **1a** and **1b** before and after UV light irradiation was measured on powdered microcrystalline samples under a constant magnetic field of 0.1 T. The χT *vs* T plots (χ is the molar paramagnetic susceptibility per Cu(II) center; Fig. S16) of compounds **1a** and **1b** show that in all cases (open or closed forms), the susceptibility follows a quasi-Curie law along the whole temperature range in agreement with non-interacting S = ½ systems (a constant value of 0.44 cm^3 K mol^{-1} for both, **1a** and **1b**, before irradiation and of 0.43 cm^3 K mol^{-1} for both complexes after the irradiation with UV light). This indicates that the diaryl ethane spacer, as expected, does not mediate any significant magnetic exchange between the metal ions. The irradiation of powdered samples of both compounds with UV light (λ = 385 nm, P = 3 mW/cm^2) using the same LEDs than the ones used for the optical reflectivity measurements, causes a change of color from green to deep violet. The absence of changes to the magnetic susceptibility in the resulting samples (Fig S16) may be a consequence that upon ring closure, the diarylethene **H_2L** spacer does not increase in any efficient way the Cu···Cu exchange interactions. In addition, one must also consider that the photoisomerization in solid state may not have taken place throughout the entire bulk of the sample but only down to a certain depth below the surface.

Conclusions

The reaction of a diarylethene photochromic dicarboxylate ligand, **H_2L,** with two different Cu(II) salts produces two different solvatomorphs of the polymeric complex [Cu(L)(py)$_3$] (**1**). These compounds do not contain any counterions introduced by the Cu salts (NO_3^- or AcO^-) but they certainly induce the disparity in the outcome of both reactions. The nature of the co-crystallized solvent (pyridine or H_2O/Et_2O) gives rise to significantly different organizations in the crystal lattice. Quite remarkably, these differences result in noticeably differing photochromic properties for these two systems. Thus, the pyridine

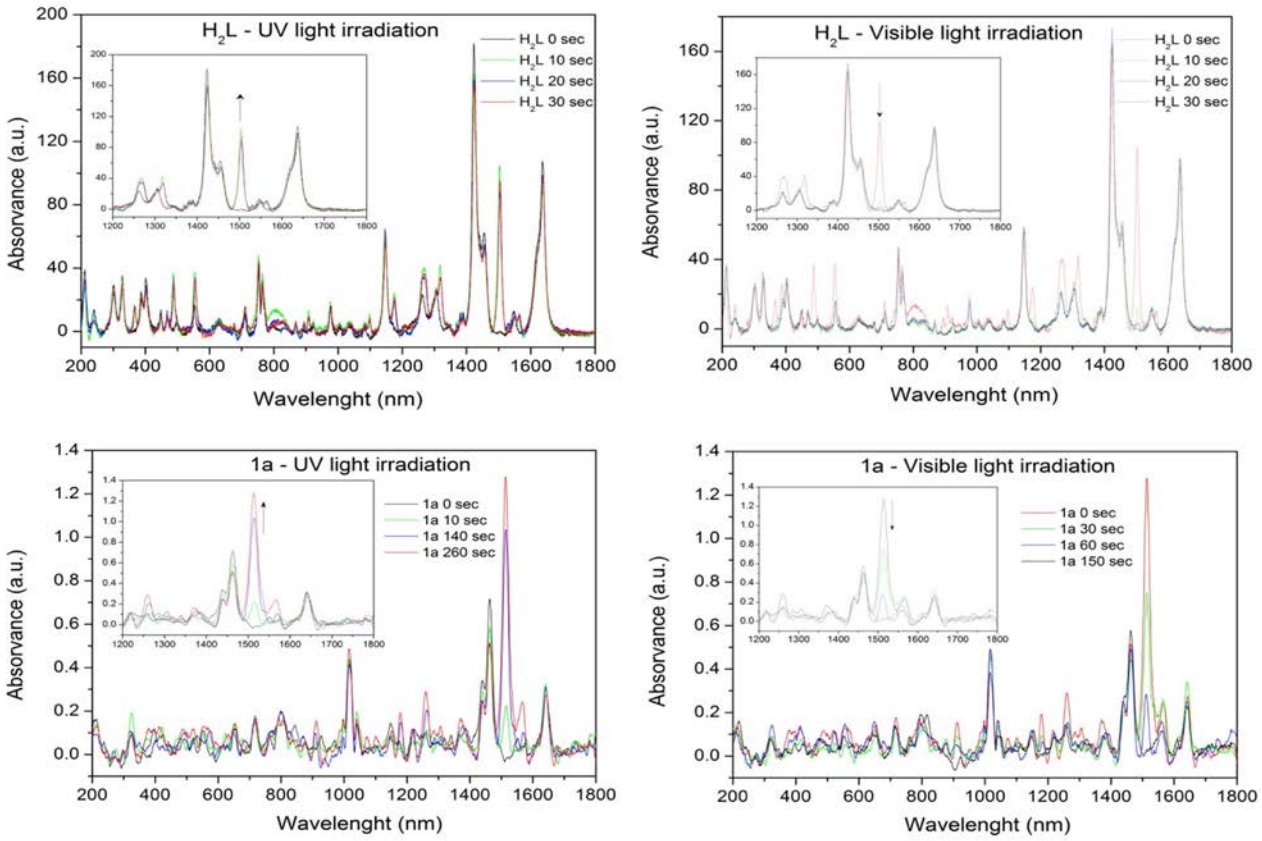

Figure 6. Evolution of the Raman spectra of the **H_2L** ligand and complex **1a** upon continuous irradiation with UV-light (λ < 425 nm) (a) and (c), respectively, and visible light (λ > 430 nm) (b) and (d), respectively, showing the reversible changes occurring upon a process of photoisomerization.

solvate, **1a**, exhibits reversible solid state ring closure photoisomerism, whereas this process is significantly hampered for the other system, **1b**, and seems to be irreversible. Thus, these results show that the subtleties of crystal engineering may constitute an avenue for modulating the photo-activity in the solid state, with potential for the understanding of these intriguing functional materials and for the design of future single crystal photochromic systems.

Experimental section

Synthesis

All chemicals were purchased from commercial sources and used without further purification. The ligand 1,2-bis(5-carboxy-2-methylthien-3-yl)cyclopentene, **H_2L**, was synthesized according to a previously reported procedure.[36] All coordination chemistry reactions were performed under aerobic conditions.

$[Cu(L)(py)_3]\cdot 2py$ (1a). A solution of **H_2L** (50 mg, 0.143 mmol) and NaH (11.46 mg, 0.286 mmol) in pyridine (15 mL) was added to a solution of $Cu(AcO)_2\cdot H_2O$ (28.66 mg, 0.143 mmol) in pyridine (15 mL). The resulting green solution was stirred for 2 hours, filtered and the filtrate was layered with ether (30 mL). After one day, blue crystals were obtained (yield 92 mg, 78%). IR (KrB pellet, cm^{-1}): 3439 b, 3108 w, 3065 w, 2904 w, 2843 w, 1600 s, 1465 s , 1447 s, 1378 s, 1334 s, 1213 m , 1147 m , 1069m , 769 s, 695 m. Anal. (found) calcd for **1a**·$3H_2O$(–2py): C, (55.25) 54.80; H, (4.70) 5.03; N, (5.38) 5.99.

$[Cu(L)(py)_3]\cdot 2H_2O\cdot 0.5Et_2O$ (1b). A solution of **H_2L** (50 mg, 0.143 mmol) and NaH (11.46 mg, 0.286 mmol) in pyridine (15 mL) was added to a solution of $Cu(NO_3)_2\cdot 3H_2O$ (33.26 mg, 0.143 mmol) in pyridine (15 mL). The resulting green solution was mixed for 2 hours, filtered and the filtrate was layered with ether (30 mL). After five days, blue crystals were collected (yield 67 mg, 66%). IR (KrB pellet, cm^{-1}): 3400 b, 2969 m, 2908 m , 2834 m, 1605 s, 1460 s, 1378 s, 1343 s, 1216 m, 1150 m, 1044 s, 875 w, 804 s, 773 s, 695 s. Anal. (found) calcd for **1b** (–0.5Et2O): C, (56.60) 56.24; H, (4.75) 4.88; N, (6.15) 6.15.

Physical measurements

The elemental analysis was performed with a Perkin-Elmer Series II CHNS/O Analyzer 2400, at the Servei de Microanàlisi of CSIC, Barcelona, Spain. IR spectra were recorded as KBr pellet samples on a Nicolet 5700 FTIR spectrometer. Raman spectra of microcrystalline samples were obtained using a Jobin-Yvon LabRam HR 800 spectrometer with a CCD camera cooled at -70 °C and an optical microscope Olympus BXFM. The Raman spectra of both the open and closed isomers were acquired with an excitation wavelength of 785 nm in order to avoid the cycloreversion reaction of the closed form isomer. The

current employed was 185 mA with the minimum power available (10 % of the total) to prevent sample damaging. Magnetic measurements were performed on freshly filtered polycrystalline samples (18.06 mg for **1a** and 10.08 mg for **1b**) introduced in a polyethylene bag (3 × 0.5 × 0.02 cm) using a Quantum Design SQUID magnetometer (MPMSXL). The corresponding irradiated compounds were prepared under air at room temperature using a light emitting diode (LED) operating at 365 nm. Surface reflectivity measurements were performed on a home-built system at different temperatures ranging from 10 to 300 K. This setup collects the light reflected by the sample (sum of direct and diffuse reflected light) that is analyzed by a high-sensitivity Hamamatsu 10083CA spectrometer. The spectra are compared to a white reference obtained with a NIST traceable standard for reflectance (SphereOptics, ref SG3054). The background, collected with the light source switched off, is subtracted from all measurements. The reflectivity can be plotted as a function of temperature, time, or wavelength. Different light emitting diodes (LEDs) operating between 365 and 1050 nm and bought from Thorlabs were used for excitation measurements. The temperature dependence of the optical reflectivity spectra was followed during a cycle of cooling–heating with a rate maintained at 4 $K \cdot min^{-1}$. The excitation/de-excitation experiments were performed between 290 and 295 K.

X-ray crystallography

Data were collected on blue (**1a**) and green (**1b**) plates using Mo Kα radiation (λ = 0.71073 Å) on a Bruker APEX II QUAZAR diffractometer equipped with a microfocus multilayer monochromator at 100 K. Data reduction and absorption corrections were performed with SAINT and SADABS. [46] The structures were solved and refined on F^2 with the SHELXTL suite. [47] All non-hydrogen atoms were refined anisotropically. The pyridine in the axial position of the copper in complex **1a** exhibits positional disorder over two locations, which was refined and established in 0.73/0.27 occupancy ratios. In complex **1b** a partial ether molecule is disordered over two positions by symmetry. Hydrogen atoms were placed geometrically on their carrier atoms and refined with a riding model where possible. Data available at the CCDC (1448770 and 1448771 for **1a** and **1b** respectively).

Acknowledgements

G.A. thanks the Generalitat de Catalunya for the prize ICREA Academia 2008 and 2013, for excellence in research and the ERC for a Starting Grant (258060 FuncMolQIP). The authors thank the Spanish MICINN for funding through MAT2011-24284 (OR) and the ERC for a Predoctoral Fellowship (JSU) under Grant 258060 FuncMolQIP. M.E. acknowledges the Spanish Ministry of Science and Innovation through the Juan de la Cierva Program. R.C. and C.M. acknowledge the University of Bordeaux, the Région Aquitaine, the ANR, the CNRS, the Institute Universitaire de France and the GdR MCM-2 : Magnétisme et Commutation Moléculaires.

Notes and references

1. E. D.-P. A. Bianchi, E. García-España, C. Giorgi, and F. Pina, *Coord. Chem. Rev.*, 2014, **260**, 156-215.
2. M. S. C. Falenczyk, B. Karaman, T. Rumpf, N. Kuzmanovic, M. Grøtli, W. Sippl, M. Jung, and B. König, *Chem. Sci.*, 2014, **5**, 4794-4799.
3. H. J. D. Kim, H. Lee, W.-T. Hwang, J. Wolf, E. Scheer, T. Huhn, H. Jeong, and T. Lee, *Adv. Mater.*, 2014, **26**, 3968-3973.
4. T. B. N. E. Murguly, and N. R. Branda, *Angew. Chem. Int. Ed.*, 2001, **40**, 1752-1755.
5. B. L. Feringa, *Molecular Switches*, Wiley-VCH, Weinheim, Germany, 2001.
6. Q. Z. J. Zhang, and H. Tian, *Adv. Mater.*, 2012, **24**, 1-22.
7. I. F. M. McCullagh, M. A. Ratner, and G. C. Schatz, *J. Am. Chem. Soc.*, 2011, **133**, 3452–3459.
8. J. J. N. Shao, H. Wang, J. Zheng, R. Yang, W. Chan, and Z. Abliz, *J. Am. Chem. Soc.*, 2010, **132**, 725-736.
9. J. Park, L.-B. Sun, Y.-P. Chen, Z. Perry and H.-C. Zhou, *Angew. Chem. Int. Ed.*, 2014, **53**, 5842-5846.
10. M. P. S.-C. Wei, K. Li, S. Wang, J. Zhang, and C.-Y. Su, *Adv. Mater.*, 2013, **26**, 2072-2077.
11. M. Singer and A. Jäschke, *J. Am. Chem. Soc.*, 2010, **132**, 8372-8377.
12. Y. X. Y. Wu, Q. Zhang, H. Tian, W. Zhu, and A. D. Q. Li, *Angew. Chem. Int. Ed.*, 2014, **53**, 1-6.
13. J. Zhang, J. Wang and H. Tian, *Materials Horizons*, 2014, **1**, 169-184.
14. E. C. G. Abellán, C. Martí-Gastaldo, A. Ribera, J. L. Jordá, and H. García, *Adv. Mater.*, 2014, **26**, 4156-4162.
15. M. Morimoto, H. Miyasaka, M. Yamashita and M. Irie, *J. Am. Chem. Soc.*, 2009, **131**, 9823-9835.
16. N. R. B. A. Peters, S. Fraser, V. Uni, V. Dri, and C. Va, *J. Am. Chem. Soc.*, 2003, **125**, 3404-3405.
17. T. K. N. Katsonis, M. Walko, S. J. van der Molen, B. J. van Wees, and B. L. Feringa, *Adv. Mater.*, 2006, **18**, 1397-1400.
18. T. F. M. Irie, T. Sasaki, N. Tamai, and T. Kawai, *Nature*, 2002, **420**, 759-760.
19. M. Irie, *Photochem. Photobiol. Sci.*, 2010, **9**, 1535-1542.
20. S. Kobatake and M. Irie, *Bull. Chem. Soc. Jpn.*, 2004, **77**, 195-210.
21. M. Irie, *Chem. Rev.*, 2000, **100**, 1685-1716.
22. S. K. M. Morimoto, and M. Irie, *Chem. Rec.*, 2004, **4**, 23-38.
23. M. Morimoto and M. Irie, *Chem. Eur. J.*, 2006, **12**, 4275-4282.
24. H. L. K. Motoyama, T. Koike, M. Hatakeyama, S. Yokojima, S. Nakamura, and M. Akita, *Dalt. Trans.*, 2011, **40**, 10643-10657.
25. T. K. K. Motoyama, and M. Akita, *Chem. Commun.*, 2008, 5812-5814.
26. Q. Z. W. Tan, J. Zhang, and H. Tian, *Org. Lett.*, 2009, **11**, 161-164.
27. J. Y. Y. Lin, M. Hu, J. Cheng, J. Yin, S. Jin, and S. H. Liu, *Organometallics*, 2009, **28**, 6402-6409.
28. M. R. D. Pinkowicz, L.-M. Zheng, S. Sato, M. Hasegawa, M. Morimoto, M. Irie, B. K. Breedlove, G. Cosquer, K. Katoh, and M. Yamashita, *Chem., Eur. J.*, 2014, **20**, 12502-12513.
29. M. M. G. Cosquer, M. Irie, A. Fetoh, B. K. Breedlove, and M. Yamashita, *Dalt. Trans.*, 2015, **44**, 5996-6002.
30. M. M. J. Han, Y. Suenaga, H. Ebisu, A. Nabei, T. Kuroda-Sowa, and M. Munakata, *Inorg. Chem.*, 2007, **46**, 3313-3321.

31. N. Z. K. Sénéchal-David, M. Walko, E. Halza, E. Rivière, R. Guillot, B. L. Feringa, and M.-L. Boillot, *Dalt. Trans.*, 2008, 1932-1936.
32. J. H. M. Munakata, M. Maekawa, Y. Suenaga, T. Kuroda-Sowa, A. Nabei, and H. Ebisu, *Inorg. Chim. Acta*, 2007, **360**, 2792-2796.
33. H. M. S. Takuya, M. Yamashita, M. Morimoto, and M. Irie, *Dalt. Trans.*, 2011, **40**, 2275-2282.
34. K. T. K. Matsuda, and M. Irie, *Inorg. Chem.*, 2004, **43**, 482-489.
35. J. H. M. Munakata, A. Nabei, T. Kuroda-Sowa, M. Maekawa, Y. Suenaga, and N. Gunjima, *Polyhedron*, 2006, **25**, 3519-3525.
36. J. J. D. d. J. L. N. Lucas, J. H. van Esch, R. M. Kellogg, and B. L. Feringa, *Eur. J. Org. Chem.*, 2003, 155-166.
37. R. Y. B. Qin, and H. Tian, *Inorg. Chim. Acta*, 2004, **357**, 3382-3384.
38. G.-A. Y. J.-T. Guan, J. Yin, Y. Lin, and S.-H. Liu, *Acta Cryst.*, 2007, **E63**, m1499-m1500.
39. G.-A. Y. J.-T. Guan, J. Yin, X.-G. Meng, and S.-H. Liu, *Acta Cryst.*, 2007, **E63**, m1515-m1516.
40. K. U. S. Kobatake, E. Tsuchida, M. Irie, and T. Corporation, *Chem. Commun.*, 2002, **2**, 2804-2805.
41. R. F. T. Nakashima, and T. Kawai, *Chem. Eur. J.*, 2011, **17**, 10951-10957.
42. R. B. R. Yasukuni, J. Grand, N. Félidj, F. Maurel, A. Perrier, R. Métivier, K. Nakatani, P. Yu, and J. Aubard, *J. Phys. Chem. C*, 2012, **116**, 16063-16069.
43. F. W. X.-H. Zhou, F.-S. Zhang, F.-Q. Zhao, X.-D. Liu, F.-Y. Xu, and C.-H. Tung, J., *Photochem. Photobiol. A,*, 2005, **171**, 205-208.
44. J. J. D. d. Jong, W. R. Browne, M. Walko, L. N. Lucas, L. J. Barrett, J. J. McGarvey, J. H. v. Esch and B. L. Feringa, *Org. Biomol. Chem.*, 2006, **4**, 2387-2232.
45. S. K. K. Saita, T. Fukaminato, S. Nanbu, M. Irie, and H. Sekiya, *Chem. Phys. Lett.*, 2008, **454**, 42-48.
46. 2014, *SAINT and SADABS*, Bruker AXS Inc., Madison, Wisconsin, USA.
47. G. M. Sheldrick, *Acta Cryst. A*, 2015, **71**, 3-8.